Uniquely Decodable Codes for Physical-Layer Network Coding in Wireless Cooperative Communications

Qi-Yue Yu, *Senior Member, IEEE*, Ya-Tian Li, Wei-Xiao Meng, *Senior Member, IEEE*, and Wei Xiang, *Senior Member, IEEE*

***Abstract*—Physical-layer network coding (PNC) has received much attention, both from academia and industry lately, since it takes advantages of multiple-access signals. Because of a reduced number of time slots (TSs), PNC is capable of improving throughput significantly, especially for a typical 3-node network consisting of 2 user terminals and 1 relay node. However, a network with M nodes ($M > 3$) and without adopting additional techniques needs ($2M - 2$) TSs to realize information exchange among all the nodes, since network coding is unable to distinguish between users at the relay node. This paper proposes uniquely decodable codes (UDCs) for PNC in wireless cooperative communications. The proposed UDC requires only two TSs for information exchange irrespective of the number of nodes in the network. This paper also investigates the amplify-and-forward and decode-and-forward modes for UDC-based PNC. The bit error rate and throughput of the proposed schemes are analyzed in this paper. Using simulation results, we demonstrate that our theoretical results align well with the simulation results.**

***Index Terms*—Cooperative communications, multiple-access channel, physical-layer network coding (PNC), uniquely decodable codes (UDCs).**

I. Introduction

NETWORK coding (NC) is used both in wired and wireless networks [1]. One of the most promising topics on NC is physical-layer NC (PNC) [2], [3], which takes advantages of multiple-access interference signals at relay node and achieves higher throughput. PNC can be viewed as a special case of cooperative communications [4]–[6].

There exists a great deal of works on PNC in literature, including but not limited to the following:

1) various coding methods for PNC [7]–[13], e.g., convolutional codes [12], repeat-accumulate codes, and low-density parity-check codes [7], [13];
2) various modulation schemes for PNC [14]–[17];
3) asynchronous problems of PNC [19]–[22].

Besides these basic physical-layer techniques, the PNC network is also an interesting research topic [23]–[25].

It is well known that the flat fading channel is more attractive and important for wireless transmission. Hence, how to reduce the effect of the Rayleigh fading channel is another important problem of PNC. Most existing works on PNC are restricted to the additive white Gaussian noise (AWGN) channel. Some of them tackle the problem in fading channels using equalization [26], pre-coding [27], [28], or multiple-input multiple-output (MIMO) techniques [29], [30]. However, the degrees of freedom brought by MIMO are not fully utilized, since extra antennas are used to overcome the Rayleigh fading.

Actually, PNC is able to significantly increase the throughput of the 3-node network. However, it is not suitable for the M-node ($M \geq 3$) network consisting of ($M - 1$) user terminals and one relay node, since NC (such as "XOR") is unable to distinguish data from multiple users. Therefore, it is an interesting problem to reduce the number of time slots (TSs) for the M-node network without degrading the throughput in the Rayleigh fading channel [18], [31].

Currently, the non-orthogonal multiple access (NOMA) technique has been widely used in PNC systems [31]–[34]. Using different power-domain and/or multiple constellations, it is possible to support multiple users to share the same resources and improve spectral efficiency. There are a variety of types of NOMA techniques, e.g., power-domain NOMA, sparse code multiple access (SCMA). Unlike power-domain NOMA, this paper exploits the application of uniquely-decodable codes (UDCs) in extracting and mapping data from multiple user terminals at the relay node. The UDC was originally designed for multiple-access channels [35]–[41]. The essential idea behind the UDC is to extract data from multiple users without ambiguity. Thus, the UDC can be viewed as a special case of NOMA, and it exploits coding techniques to separate different users. The achievable data rate of UDCs is higher than the largest rate of any single user, and some UDCs can even correct errors in a noisy channel [37]. Inspired by these attractive features of UDCs, this paper is the first to integrate UDCs into PNC. The main contributions of this paper can be summarized as follows.

1) This paper proposes new UDC-based PNC schemes both for the amplify-and-forward (AF) and decode-and-

Manuscript received June 26, 2018; revised October 25, 2018 and December 5, 2018; accepted January 4, 2019. Date of publication February 13, 2019; date of current version November 22, 2019. This work was supported by the National Natural Science Foundation of China under Grants 61671171 and 91438205. *(Corresponding author: Qi-Yue Yu.)*

Q.-Y. Yu and W.-X. Meng are with the Communication Research Center, Harbin Institute of Technology, Harbin 150001, China (e-mail: yuqiyue@hit.edu.cn; wxmeng@hit.edu.cn).

Y.-T. Li is with the Lab of Laser Communication, Changchun Institute of Optics, Fine Mechanics and Physics, Chinese Academy of Sciences, Changchun 130033, China (e-mail: yt_li@ciomp.ac.cn).

W. Xiang is with the College of Science and Engineering, James Cook University, Cairns, Queens. 4870, Australia (e-mail: wei.xiang@jcu.edu.au).

Digital Object Identifier 10.1109/JSYST.2019.2891785

forward (DF) modes, and investigates the transmitter and receiver structures of the proposed system.

2) The theoretical bit error rate (BER) and the throughput performances of the proposed system are derived in detail.
3) A UDC-based multi-user PNC scheme, as well as a corresponding pre-coding technique, is proposed.

The remainder of this paper is organized as follows. The basic architecture of UDC-based PNC is presented in Section II. A special class of UDC for the proposed schemes is presented in Section III. The BER and the throughput for the given models are analyzed theoretically in Section IV. UDC-based multiple-user PNC and pre-coding techniques for the proposed scheme are discussed in Section V. Simulation results are presented in Section VI. Finally, some concluding remarks and future work are offered in Section VII.

II. Architecture of UDC-Based PNC

In this paper, it is assumed that there are no direct communication links between any two users. They have to exchange information via any relay node. It is also supposed that BPSK is adopted during the entire transmission.

A. Traditional NC and PNC for the 3-Node Network

Consider a general 3-node network model, which includes two user terminals (users 1 and 2) and one relay node (node R). Actually, any one of networks can be decomposed into a number of basic 3-node networks; therefore, the 3-node model is focused upon in this research. As illustrated in Fig. 1(a), the traditional scheme needs four TSs to complete information exchange. Considering the NC scheme in Fig. 1(b), the data sequences $d_1(t)$ of user 1 and $d_2(t)$ of user 2 are modulated to signals $s_1(t)$ and $s_2(t)$, and then are sent to relay node R during the first and second TSs, respectively. Then, NC is carried out at the relay node, i.e., $d_R(t) = d_1(t) \oplus d_2(t)$, and the NC-encoded $d_R(t)$ is modulated to $s_R(t)$, which is then broadcast to the two user terminals in the third TS. Users 1 and 2 can obtain $d_2(t) = d_1(t) \oplus (d_1(t) \oplus d_2(t))$ and $d_1(t) = d_2(t) \oplus (d_1(t) \oplus d_2(t))$, respectively. Thus, the NC scheme needs three TSs to complete information exchange. For the PNC scheme, two users simultaneously send their signals during the first TS. Assuming perfect synchronization, the relay node R receives the sum-signal $(s_1(t) + s_2(t))$ of the two users. After mapping the sum-signal into the encoded data $d_R(t) = d_1(t) \oplus d_2(t)$, relay node R broadcasts the PNC signal [as shown in Fig. 1(c)]. Thus, the PNC scheme needs only two TSs to complete information exchange.

B. UDC-Based PNC for the 3-Node Network

This paper presents two types of UDC-based PNC schemes for the 3-node network. These two schemes are elaborated as follows.

1) UDC-Based AF PNC Scheme: The frame of the AF mode is shown in Fig. 2, and the system block diagram is shown in Fig. 3.

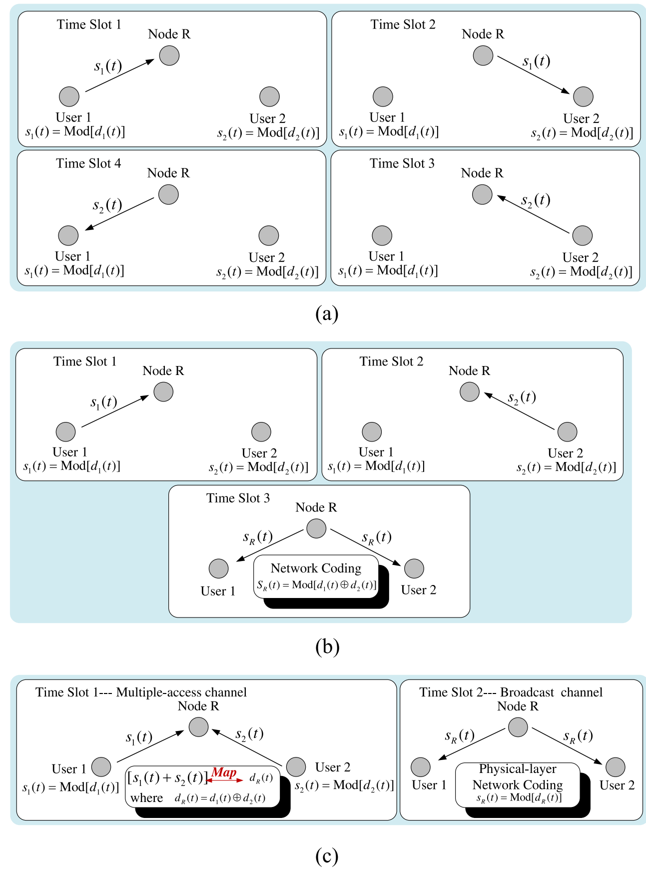

Fig. 1. Traditional, NC, and PNC schemes, where "Mod" and "Map" represent modulation and mapping, respectively. (a) Traditional scheme. (b) NC scheme. (c) PNC scheme.

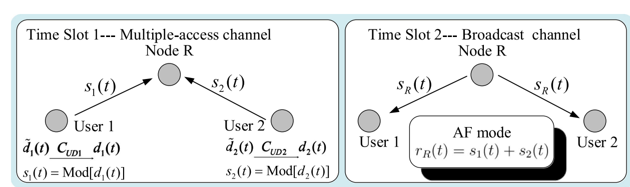

Fig. 2. UDC-based AF PNC scheme.

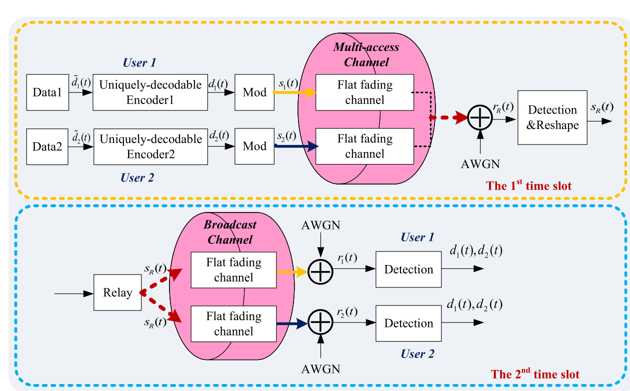

Fig. 3. Transceiver diagram of the UDC-based AF PNC scheme.

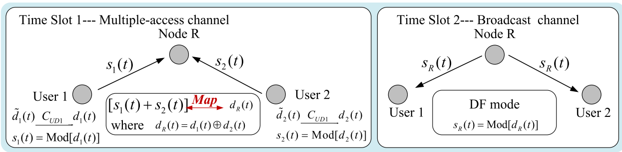

Fig. 4. UDC-based DF PNC scheme.

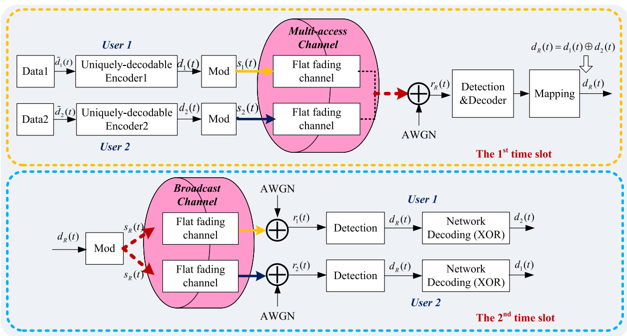

Fig. 5. Transceiver diagram of the UDC-based DF PNC scheme.

This scheme consists of two TSs. During the first TS, two separate user terminals simultaneously transmit data sequences to the relay node, denote by $\tilde{d}_1(t)$ and $\tilde{d}_2(t)$. In the first TS, $\tilde{d}_1(t)$ and $\tilde{d}_2(t)$ pass through UDC encoders C_1 and C_2, yielding encoded data sequences $d_1(t)$ and $d_2(t)$, respectively. The encoded data $d_1(t)$ and $d_2(t)$ are then modulated into $s_1(t)$ and $s_2(t)$ apiece. Next, the modulated signals $s_1(t)$ and $s_2(t)$ are transmitted through two separate flat fading channels. The relay node directly forwards the combined sum-signal with only some simple signal processing, i.e., decision. In the second TS, the relay node broadcasts the combined sum-signal to the two user terminals.

This scheme has three major features in comparison to its conventional PNC counterpart. First of all, the sum data rate at the relay node, $R_1 + R_2$, is greater than 1 and smaller than 2, where R_1 and R_2 are the rates of users 1 and 2, respectively. This will be further introduced in the following section. Since the relay node in this scheme only decodes and forwards the received combined sum-signal, this does not change the data rate. Second, the UDC decoding table is required at each terminal node. Third, this scheme is unable to take advantages of the error detection (or correction) feature of UDC, since the relay node does not perform UDC decoding.

2) UDC-Based DF PNC Scheme: Fig. 4 illustrates the UDC-based DF PNC scheme. Actually, this scheme can be seen as a special case of PNC, since the only difference is that UDC encoding is performed before modulation as shown in Fig. 5. Consequently, the relay node needs to first detect the sum-signal and then map the detected signal with NC, i.e., $d_R(t) = d_1(t) \oplus d_2(t)$.

Aided by UDC, this scheme is capable of improving the BER. Moreover, it is applicable to not only the AWGN channel but also the flat fading channel. The UDC decoding table is only needed at the relay node, whereas in the AF PNC case it is needed at each user terminal. This helps reduce the design complexity of the receiver.

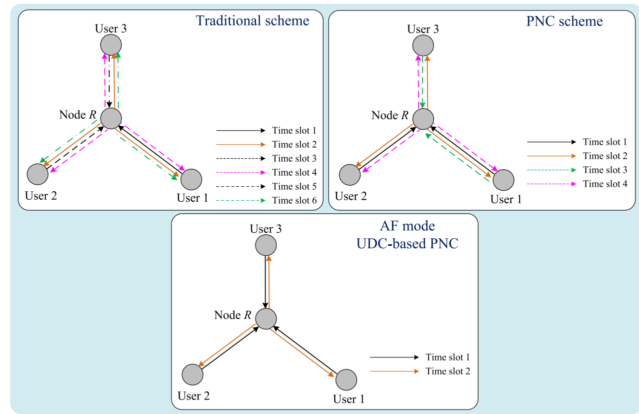

Fig. 6. Traditional, PNC, and UDC-based AF PNC of a 4-node network.

C. Multiple-Node Network

For a multiple-node network with M user terminals and one relay node, assuming there are no direct links between any two users, the traditional non-NC scheme needs $2M$ TSs for information exchange. For PNC, the smallest number of TSs is $2M - 2$. Take the 4-node network shown in Fig. 6 as an example. In the first TS, users 1 and 2 send signals to relay node R, which then broadcasts the network-coded signal to all the nodes in the second TS. Hence, users 1 and 2 are able to obtain each other's information after the second TS. During the third TS, users 1 and 3 send signals to the relay node, which broadcasts the network-coded signal in the fourth TS. User 3 recovers user 1's information in the fourth TS, and then obtains user 2's information according to the received signal of the first TS. Similarly, user 2 can recover the information from user 3 by using the information from user 1. Therefore, it is easy to see that the difference between the traditional and PNC schemes is insignificant with the increase in M.

Because multiple-user UDC can separate multiple users simultaneously, the UDC-based schemes with both the AF and DF modes are able to exchange information in two TSs for an M-node ($M > 2$) network. Because of the significantly reduced number of TSs, AF/DF provides a higher throughput than that provided by PNC. The challenge lies in the design of effective multiple-user UDCs. There have been some reported studies on multiple-user UDC [42]–[44]. However, this still remains an open research problem.

III. Special Class of the Proposed Schemes

A. Uniquely Decodable Codes

UDC is proposed for the multiple-access channel [36], in which multiple information sequences from independent users are encoded and combined into a single sequence. At the receiver, the decoder separates this coded sequence into the original sequences of the multiple users. Thereby, the coded sequence must possess a structural property such that it can be uniquely separated. The key issue of UDC is to construct UDCs for users.

Suppose V_n is the vector space of all the n-tuples over GF(2), and C_m is a subset of V_n. Denote the number of codewords in C_m by $|C_m|$. If and only if, two different n-tuple vectors

TABLE I
DECODING TABLE FOR UNIQUELY DECODABLE PAIR, $C_1 = \{00, 11\}$ AND $C_2 = \{00, 01, 10\}$

			C_1			
			0	0	1	1
C_2	0	0	0	0	1	1
	0	1	0	1	1	2
	1	0	1	0	2	1

$\mathbf{u}_m, \mathbf{v}_m \in C_m$ satisfy the following condition:

$$\sum_{m=1}^{M} \mathbf{u}_m \neq \sum_{m=1}^{M} \mathbf{v}_m \tag{1}$$

then, set C_m is supposed to constitute the UDC codewords of the mth user.

Sum rate R_{sum} is defined as

$$R_{\text{sum}} = \frac{1}{n}\log_2 \prod_{m=1}^{M} |C_m|. \tag{2}$$

Consider a simple case where the code length is $n = 2$, and the UDCs for users 1 and 2 are $C_1 = \{00, 11\}$ and $C_2 = \{00, 01, 10\}$ with the decoding table given in Table I. The rate pair for C_1 and C_2 is (0.5, 0.7925). By looking up Table I, any received vector can be decoded into two codewords C_1 and C_2 without ambiguity.

In this section, we take the given UDC pair listed in Table I as an example to elaborate on the theory behind our proposed schemes. The encoded vector set for users 1 and 2 are $\mathbf{d}_1 = (d_1(0), d_1(1)) \in \{00, 11\}$ and $\mathbf{d}_2 = (d_2(0), d_2(1)) \in \{00, 01, 10\}$, respectively. Although this UDC pair is simple, yet it provides high data rates and is instrumental in understanding the principles behind UDC.

B. AF Mode

The diagram of the UDC-based AF PNC scheme is shown in Fig. 3. Since BPSK is assumed, the modulated signal of the uth user $s_u(t)(t = 0, \ldots, n-1)$ can be expressed as

$$s_u(t) = \sqrt{E_c}\,(2d_u(t) - 1) \tag{3}$$

where $u = 1$ or 2, E_c is the symbol power in one symbol time, and $\mathbf{s}_u = (s_u(0), s_u(1), \ldots, s_u(n-1))$.

Let us first consider the case without AWGN and Rayleigh fading. The received signal $r_R(t)$ at the relay node R becomes $r_R(t) = s_1(t) + s_2(t)$. The detailed results are shown in Table II.

Then, we consider the case with flat fading. It is assumed that the channel impulse response remains constant during a single codeword interval. In this case, the time interval of a codeword equals that of two symbol intervals, since the codeword length is $n = 2$. Without consideration of AWGN, the received signal at the relay node is given by $r_R(t) = h_1 s_1(t) + h_2 s_2(t)$. For convenience of notation, we define the following:

$$\begin{cases} x = \sqrt{E_c}\,(h_1 + h_2) \\ y = \sqrt{E_c}\,(h_1 - h_2). \end{cases} \tag{4}$$

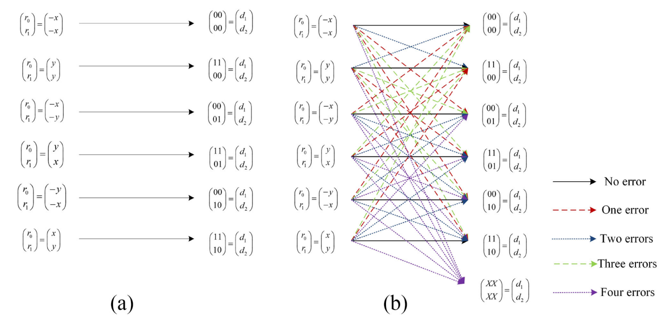

Fig. 7. Mapping process of the UDC-based AF PNC scheme. (a) Without noise. (b) With noise.

Suppose $s_R(t)$ is the result of $r_R(t)$ after decision, and is broadcast in the second TS. For simplicity, define the mapping set Ψ as the detected codeword in the noiseless channel, and $|\Psi|$ denotes the cardinality of Ψ. Apparently, there is a one-to-one correspondence between Ψ and the users. As shown in Table III, there are $|\Psi| = 6$ elements in Ψ, and $\Psi = \{\psi_1, \psi_2, \psi_3, \psi_4, \psi_5, \psi_6\} = \{(x, x), (y, y), (-x, -y), (y, x), (-y, -x), (x, y)\}$.

It may occur that $s_R(t)$ does not belong to Ψ when performing hard-decision, resulting in erasure symbols (ξ, ξ) at the relay node that will be broadcast in the second TS. The mapping set Ψ is utilized for decoding at the user nodes so that the data sequences transmitted by different users can be decoded without ambiguity. We use a simple hard-decision example to elaborate on the decoding procedure at the user node in the second TS. If the received signal is (x, y), then $\mathbf{d}_1 = (1, 1)$ and $\mathbf{d}_2 = (1, 0)$ are decoded. If the received signal falls outside of Ψ, then it is considered that the erasure symbols (ξ, ξ) are received by both users.

However, $s_R(t)$ can always be decoded inside set Ψ using soft decision, based upon the minimum Euclidean distance criterion. The mapping progress under the AF mode is illustrated in Fig. 7.

C. DF Mode

"XOR" is adopted as the mapping operation at the relay node R, i.e., $d_R(t) = d_1(t) \oplus d_2(t)$. Denote the data sequence after mapping by a vector $\mathbf{d}_R = (d_R(0), \ldots, d_R(n-1))$ with the UDC codeword length of n, which equals 2 in our case. The mapping process is presented in Table IV.

Table IV establishes a mapping relationship between the received sum-signal vector $\mathbf{r}_R = (r_R(0), r_R(1))$ and data sequence $\mathbf{d}_R$. Fig. 8 shows the mapping process without the AWGN. The relationship is given as.

1) If received signal $\mathbf{r}_R = (-x, -x)$, then $\mathbf{d}_R = (0, 0)$.
2) If received signal $\mathbf{r}_R = (y, y)$, then $\mathbf{d}_R = (1, 1)$.
3) If received signal $\mathbf{r}_R = (-x, -y)$, then $\mathbf{d}_R = (0, 1)$.
4) If received signal $\mathbf{r}_R = (y, x)$, then $\mathbf{d}_R = (1, 0)$.
5) If received signal $\mathbf{r}_R = (-y, -x)$, then $\mathbf{d}_R = (1, 0)$.
6) If received signal $\mathbf{r}_R = (x, y)$, then $\mathbf{d}_R = (0, 1)$.

When noise is included, the received signal at R will become as follows:

$$r_R(t) = h_1 s_1(t) + h_2 s_2(t) + n(t) \tag{5}$$

where $n(t)$ is the Gaussian noise with variance σ^2.

TABLE II
RECEIVED SIGNAL AT THE RELAY NODE WITHOUT CONSIDERING FLAT FADING

		User 1	
		$(s_1(0), s_1(1)) = (-\sqrt{E_c}, -\sqrt{E_c})$	$(s_1(0), s_1(1)) = (\sqrt{E_c}, \sqrt{E_c})$
User 2	$(s_2(0), s_2(1)) = (-\sqrt{E_c}, -\sqrt{E_c})$	$(r_0, r_1) = (-2\sqrt{E_c}, -2\sqrt{E_c})$	$(r_0, r_1) = (0, 0)$
	$(s_2(0), s_2(1)) = (-\sqrt{E_c}, \sqrt{E_c})$	$(r_0, r_1) = (-2\sqrt{E_c}, 0)$	$(r_0, r_1) = (0, 2\sqrt{E_c})$
	$(s_2(0), s_2(1)) = (\sqrt{E_c}, -\sqrt{E_c})$	$(r_0, r_1) = (0, -2\sqrt{E_c})$	$(r_0, r_1) = (2\sqrt{E_c}, 0)$

TABLE III
RECEIVED SIGNAL AT THE RELAY NODE IN CONSIDERATION OF FLAT FADING

		User 1	
		$(s_1(0), s_1(1)) = (-\sqrt{E_c}, -\sqrt{E_c})$	$(s_1(0), s_1(1)) = (\sqrt{E_c}, \sqrt{E_c})$
User 2	$(s_2(0), s_2(1)) = (-\sqrt{E_c}, -\sqrt{E_c})$	$(r_0, r_1) = (-x, -x)$	$(r_0, r_1) = (y, y)$
	$(s_2(0), s_2(1)) = (-\sqrt{E_c}, \sqrt{E_c})$	$(r_0, r_1) = (-x, -y)$	$(r_0, r_1) = (y, x)$
	$(s_2(0), s_2(1)) = (\sqrt{E_c}, -\sqrt{E_c})$	$(r_0, r_1) = (-y, -x)$	$(r_0, r_1) = (x, y)$

TABLE IV
DATA SEQUENCE MAPPING AT RELAY NODE R USING "XOR"

		User 1	
		$\mathbf{d}_1 = (0, 0)$	$\mathbf{d}_1 = (1, 1)$
User 2	$\mathbf{d}_2 = (0, 0)$	$\mathbf{d}_R = (0, 0)$	$\mathbf{d}_R = (1, 1)$
	$\mathbf{d}_2 = (0, 1)$	$\mathbf{d}_R = (0, 1)$	$\mathbf{d}_R = (1, 0)$
	$\mathbf{d}_2 = (1, 0)$	$\mathbf{d}_R = (1, 0)$	$\mathbf{d}_R = (0, 1)$

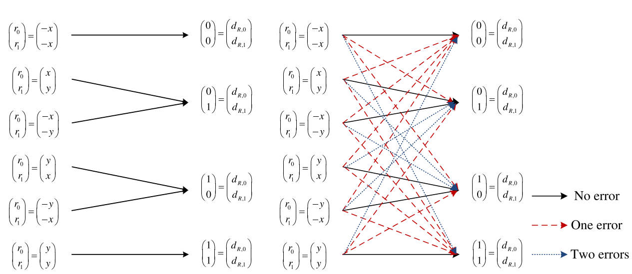

(a) (b)

Fig. 8. Mapping process of the UDC-based DF PNC scheme. (a) Without noise. (b) With noise.

Noise will cause mapping errors. For example, assume that the correctly detected signal vector is $(-x, -x)$; if there are no mapping errors, the mapped output vector will be $(0, 0)$. With one mapping error, the mapped output will be either $(0, 1)$ or $(1, 0)$, whereas the output is $(1, 1)$ if there are two mapping errors. The mapping process of the UDC-based DF PNC scheme in a noisy channel is illustrated in Fig. 8.

After obtaining the mapped data sequence $d_R(t)$, it is then modulated into $s_R(t)$ and broadcast to both users 1 and 2.

At each user terminal, users 1 and 2 perform $d_2(t) = d_1(t) \oplus (d_1(t) \oplus d_2(t))$ and $d_1(t) = d_2(t) \oplus (d_1(t) \oplus d_2(t))$, respectively, to complete information exchange.

IV. THEORETICAL ANALYSIS OF THE PROPOSED SCHEMES

In this section, we will analyze the symbol error rate (SER) of the proposed schemes with the AF and DF modes. It is assumed that the channel state information (CSI) is perfectly known at both the transmitters and receivers, and that BPSK modulation is used. Meanwhile, there are no sysnchronization errors, and 0 s and 1 s are generated with equiprobability by each user.

A. General SER Analysis

The end-to-end system SERs of the proposed schemes are determined both by the first TS (multiple-access phase) and the second TS (broadcast phase).

We first discuss the first TS. Without loss of generality, we assume $|h_1|^2 > |h_2|^2 > 0$. It is noted that the probability of $|h_1|^2 = |h_2|^2$ is extremely small, and thus negligible for a random fading channel. The received signal at the relay node can be expressed as (6), shown at the bottom of this page.

Denote by $p_{a\to b} (= P(b|a))$ the probability of detected symbol b, given that symbol a is transmitted. $f(r\,|x)$, $f(r\,|y)$,

$$
\begin{aligned}
r_R(t) &= h_1 s_1(t) + h_2 s_2(t) + n(t)\\
&= \begin{cases}
\sqrt{E_c}h_1 + \sqrt{E_c}h_2 + n(t) = x + n(t), & \text{if } s_1(t) = \sqrt{E_c}, s_2(t) = \sqrt{E_c}\\
\sqrt{E_c}h_1 - \sqrt{E_c}h_2 + n(t) = y + n(t), & \text{if } s_1(t) = \sqrt{E_c}, s_2(t) = -\sqrt{E_c}\\
-\sqrt{E_c}h_1 + \sqrt{E_c}h_2 + n(t) = -y + n(t), & \text{if } s_1(t) = -\sqrt{E_c}, s_2(t) = \sqrt{E_c}\\
-\sqrt{E_c}h_1 - \sqrt{E_c}h_2 + n(t) = -x + n(t), & \text{if } s_1(t) = -\sqrt{E_c}, s_2(t) = -\sqrt{E_c}
\end{cases}
\end{aligned}
\tag{6}
$$

$f(|h_1|^2)$, and $f(|h_2|^2)$ are defined as the probability density functions (PDFs) given by

$$\begin{aligned} f(r\,|x) &= \frac{1}{\sqrt{2\pi}\sigma}\exp\left\{-\frac{\left[r-\sqrt{E_c}\,(h_1+h_2)\right]^2}{2\sigma^2}\right\} \\ f(r\,|y) &= \frac{1}{\sqrt{2\pi}\sigma}\exp\left\{-\frac{\left[r-\sqrt{E_c}\,(h_1-h_2)\right]^2}{2\sigma^2}\right\} \\ f(|h_1|^2) &= \frac{|h_1|^2}{\sigma_{\text{Ray}}^2}\exp\left(-\frac{\left(|h_1|^2\right)^2}{2\sigma_{\text{Ray}}^2}\right) \\ f(|h_2|^2) &= \frac{|h_2|^2}{\sigma_{\text{Ray}}^2}\exp\left(-\frac{\left(|h_2|^2\right)^2}{2\sigma_{\text{Ray}}^2}\right) \end{aligned} \tag{7}$$

where $|h_1|^2$ and $|h_2|^2$ follow the same Rayleigh distribution with variance σ_{Ray}^2.

It is easy to see that the optimal decision thresholds for the given scheme are respectively $h_1\sqrt{E_c}$, 0 and $-h_1\sqrt{E_c}$, owing to the facts that the transmit signals are of equiprobability and BPSK modulated. Thus, we arrive at (8), shown at the bottom of this page, where we have the following:

$$P = \iint_{|h_1|^2>|h_2|^2} f(|h_1|^2)f(|h_2|^2)\mathrm{d}|h_1|^2\mathrm{d}|h_2|^2$$

Because of the symmetry between x and $-x$, it is easy to show that

$$\begin{cases} p_{(-x)\to(-y)} = p_{x\to y} \\ p_{(-x)\to y} = p_{x\to(-y)} \\ p_{(-x)\to x} = p_{x\to(-x)} \\ p_{(-x)\to(-x)} = p_{x\to x}. \end{cases} \tag{9}$$

Similarly, we have (10), as shown at the bottom this page, where

$$\begin{cases} p_{(-y)\to(-x)} = p_{y\to x} \\ p_{(-y)\to y} = p_{y\to(-y)} \\ p_{(-y)\to x} = p_{y\to(-x)} \\ p_{(-y)\to(-y)} = p_{y\to y}. \end{cases} \tag{11}$$

For further discussions, define $p_{\psi_i\to\psi_j}(=P(\psi_j|\psi_i))$ as the probability that detects codeword ψ_i as ψ_j, where $\psi_i(\psi_j)\in\Psi$. It is easy to derive the expression of $p_{\psi_i\to\psi_j}$, according to the expressions of $p_{a\to b}$. For example, assuming $\psi_i=(-x,-x)$ and $\psi_j=(x,y)$, we have $p_{\psi_i\to\psi_j}=p_{(-x)\to(x)}p_{(-x)\to(y)}$.

In the second TS, $s_R(t)$ is broadcast to the two users, and the received signal by the uth, user $r_u(t)$, is given as

$$r_u(t) = h_{Ru}s_R(t) + n_u(t) \tag{12}$$

where h_{Ru} is the channel gain between the relay node and the uth user in the second TS, and $n_u(t)$ is the AWGN. It can be readily shown that the SER of the second TS, $P_{e,\text{BC}}$,

$$\begin{aligned} p_{x\to y} &= P(y\,|x) = \frac{1}{P}\iint_{|h_1|^2>|h_2|^2}\left[\int_0^{h_1\sqrt{E_c}} f(r\,|x)\mathrm{d}r\right]f(h_1)f(h_2)\mathrm{d}h_1\mathrm{d}h_2 \\ p_{x\to(-y)} &= P(-y\,|x) = \frac{1}{P}\iint_{|h_1|^2>|h_2|^2}\left[\int_{-h_1\sqrt{E_c}}^0 f(r\,|x)\mathrm{d}r\right]f(h_1)f(h_2)\mathrm{d}h_1\mathrm{d}h_2 \\ p_{x\to(-x)} &= P(-x\,|x) = \frac{1}{P}\iint_{|h_1|^2>|h_2|^2}\left[\int_{-\infty}^{-h_1\sqrt{E_c}} f(r\,|x)\mathrm{d}r\right]f(h_1)f(h_2)\mathrm{d}h_1\mathrm{d}h_2 \\ p_{x\to x} &= P(x\,|x) = \frac{1}{P}\iint_{|h_1|^2>|h_2|^2}\left[\int_{h_1\sqrt{E_c}}^{+\infty} f(r\,|x)\mathrm{d}r\right]f(h_1)f(h_2)\mathrm{d}h_1\mathrm{d}h_2 \end{aligned} \tag{8}$$

$$\begin{aligned} p_{y\to x} &= P(x\,|y) = \frac{1}{P}\iint_{h_1>h_2}\left[\int_{h_1\sqrt{E_c}}^{+\infty} f(r\,|y)\mathrm{d}r\right]f(h_1)f(h_2)\mathrm{d}h_1\mathrm{d}h_2 \\ p_{y\to(-y)} &= P(-y\,|y) = \frac{1}{P}\iint_{h_1>h_2}\left[\int_{-h_1\sqrt{E_c}}^0 f(r\,|y)\mathrm{d}r\right]f(h_1)f(h_2)\mathrm{d}h_1\mathrm{d}h_2 \\ p_{y\to(-x)} &= P(-x\,|y) = \frac{1}{P}\iint_{h_1>h_2}\left[\int_{-\infty}^{-h_1\sqrt{E_c}} f(r\,|y)\mathrm{d}r\right]f(h_1)f(h_2)\mathrm{d}h_1\mathrm{d}h_2 \\ p_{y\to y} &= P(y\,|y) = \frac{1}{P}\iint_{h_1>h_2}\left[\int_0^{h_1\sqrt{E_c}} f(r\,|y)\mathrm{d}r\right]f(h_1)f(h_2)\mathrm{d}h_1\mathrm{d}h_2 \end{aligned} \tag{10}$$

can be obtained as

$$P_{e,\mathrm{BC}} = \int \frac{1}{2}\,\mathrm{erfc}\left(\sqrt{\frac{E_c(h_{Ru})^2}{2\sigma^2}}\right) \cdot \left[\frac{h_{Ru}}{\sigma_{\mathrm{Ray}}^2}\exp\left(-\frac{{h_{Ru}}^2}{2\sigma_{\mathrm{Ray}}^2}\right)\right] \mathrm{d}h_{Ru}. \tag{13}$$

Actually, the end-to-end system SER, P_e, consists of two parts corresponding to the multiple-access channel (first TS) and the broadcast channel (second TS), respectively. As a result, we have the following:

$$P_e = 1 - (1 - P_{e,\mathrm{MAC}})\,(1 - P_{e,\mathrm{BC}}) \tag{14}$$

where $P_{e,\mathrm{MAC}}$ is the SER of the multiple-access channel.

B. SER of the AF Mode

We discuss the SERs of the AF mode both with the soft-decision and hard-decision cases.

1) SER Upper Bound of Soft Decision: For ease of exposition, define $N_{\psi_i \to \psi_j}$ as the number of symbol errors when codeword ψ_i is erroneously detected as ψ_j. It is obvious that $1 \leq N_{\psi_i \to \psi_j} \leq n$. Let P_{out} be the probability that $\mathbf{s}_R$ is detected outside Ψ.

There exist three detection scenarios. The first scenario is that the codeword is correctly recovered. The second one is that s_R is wrongly detected to be a codeword in Ψ, while the last scenario is that s_R is detected as a codeword outside Ψ.

Thanks to the above three detection scenarios and two TSs of information exchange completion, there are nine cases in total when analyzing the system SER. Assume that the correctly detected codeword is ψ_i, while ψ_j and ψ_k $(j \neq k)$ are the erroneously detected codewords. The nine cases are discussed in detail in the following.

1) The detected codeword of the first TS corresponds to the first case, which means the detected codeword is ψ_i. If the detected codeword of the second TS is also case one, there is no detected error. If the detected codeword of the second TS belongs to case two, the detected codeword is ψ_j and the corresponding symbol errors are $N_{\psi_i \to \psi_j}$. If the detected codeword of the second TS is case three, the final detected codeword is viewed as erasure codeword (ξ, ξ) implying two symbol errors. Thus, at this time, the average SER, P_1, is derived as

$$P_1 = \sum_{i=1}^{|\Psi|} \frac{1}{|\Psi|} \cdot \frac{p_{\psi_i \to \psi_i}}{1 - P_{\text{out}}} \left(\sum_{j=1, j\neq i}^{|\Psi|} \frac{1}{n} P_{\psi_i \to \psi_j} \cdot N_{\psi_i \to \psi_j} + P_{\text{out}} \right). \tag{15}$$

2) The detected codeword in the first TS corresponds to case two, which means the detected codeword is ψ_j. If the detected codeword of the second TS is case one, there are no further errors, and the corresponding symbol errors are still $N_{\psi_i \to \psi_j}$. If the detected codeword of the second TS is $\psi_k (k \neq j)$, no error occurs when $k = i$, and $N_{\psi_j \to \psi_k}$ errors occur when $k \neq i$. Similarly, P_{out} is the probability of ψ_j being out of Ψ after the decision. Thus, the average SER, P_2, is given as:

$$P_2 = \sum_{i=1}^{|\Psi|} \sum_{j=1}^{|\Psi|} \frac{1}{|\Psi|} \cdot \frac{p_{\psi_i \to \psi_j}}{1 - P_{\text{out}}} \left(\sum_{k=1, k\neq i}^{|\Psi|} \frac{1}{n} p_{\psi_j \to \psi_k} \cdot N_{\psi_j \to \psi_k} + P_{\text{out}} \right). \tag{16}$$

When soft decision is considered at the relay, all the received codewords can find a corresponding codeword in Ψ by using the minimum Euclidean distance. There is no detected codeword outside mapping table set, Ψ. Thus, we can derive an upper bound of the average SER as $P_{e,\mathrm{AF}} = P_1 + P_2$.

2) Hard Decision: For convenience, we use the codeword error rate (CWER), P_{cw}, to approximate the SER, P_e, for the hard-decision situation. Since an arbitrary symbol error in a codeword can result in an incorrect codeword; thus, the relationship between the CWER and the SER is given as $P_e \leq P_{\text{cw}} \leq nP_e$. For the proposed case of $n = 2$, we have $P_e \approx P_{\text{cw}}$. Define the CWERs of the multiple-access and broadcast channels as $P_{\text{cw,MAC}}$ and $P_{\text{cw,BC}}$, respectively. The SER of the AF mode can be shown as

$$\begin{aligned} P_{\text{cw}} &= 1 - (1 - P_{\text{cw,MAC}})\,(1 - P_{\text{cw,BC}}) \\ &= 1 - \sum_{i=1}^{|\Psi|} \frac{1}{|\Psi|} p_{\psi_i \to \psi_i} \sum_{i=1}^{|\Psi|} \frac{1}{|\Psi|} p_{\psi_i \to \psi_i}. \end{aligned} \tag{17}$$

C. SER of the DF Mode

For the DF mode, the SER of the broadcast channel, $P_{e,\mathrm{BC}}$, is similar to (13), since the users can directly recover the received data sequences without using the mapping table. Thus, it is only necessary to discuss the $P_{e,\mathrm{MAC}}$ part of the SER of the multiple-access channel, which is determined by the mapping table.

1) SER Upper Bound of Soft Decision: Similar to the AF mode, there are two cases for the detected codewords in the first TS when employing soft decision. The first one is correct detection, while the other one is incorrectly detected codewords that are located in set Ψ. Thus, $P_{e,\mathrm{MAC}}$ can be calculated as

$$P_{e,\mathrm{MAC}} = \sum_{i=1}^{|\Psi|} \frac{1}{|\Psi|} \sum_{j=1}^{|\Psi|} \frac{1}{n} \frac{p_{\psi_i \to \psi_j}}{1 - p_{\text{out}}} N_{\psi_i \to \psi_j}. \tag{18}$$

Plugging (18) into (14), we are able to derive the average SER, $P_{e,\mathrm{DF,soft}}$, as

$$P_{e,\mathrm{DF,soft}} = 1 - (1 - P_{e,\mathrm{MAC}})\,(1 - P_{e,\mathrm{BC}}) \tag{19}$$

2) Hard Decision: The main difference between the hard decision and the soft decision is that $s_R(t)$ may be decoded out of the mapping table set, Ψ. When the detected codeword falls outside the mapping table set, Ψ, the erasure codeword (ξ, ξ) is achieved at the relay node, which will be sent out in the second TS. Although there exists a probability that detected $\mathbf{r}_u = (r_u(0), r_u(1))$ may fall into the mapping table set, Ψ, again in the second TS, yet this probability is so small that it can be ignored. Under such conditions, the average SER of the

DF mode is given as:

$$P_{e,\mathrm{DF,hard}} = \sum_{i=1}^{|\Psi|} \frac{1}{|\Psi|} \left[(1 - P_{\mathrm{out}})\, P_{e,DF,\mathrm{soft}} + P_{\mathrm{out}} \right]. \tag{20}$$

V. General Case for the Proposed Scheme

In previous sections, we discussed the UDC-based PNC schemes based upon a simple and efficient UDC and BPSK modulation. To generalize the proposed systems, where $M > 2$, the architecture of the transmitter and the receiver should be similar. It should be noted that a δ-decodable UDC is able to correct $\lfloor(\delta-1)/2\rfloor$ or fewer errors, and thus improves the SER performance. Moreover, different modulation schemes may also affect the performance. The generalized UDC-based PNC system based upon a general δ-decodable pair in conjunction with higher order modulation is capable of providing a much better performance.

In this section, multiple-user UDC-based PNC and pre-coding technique are introduced. It is noted that part of the multiple-user UDC-based PNC has been introduced in [47].

A. Multiple-User UDC-Based PNC

To realize multiple-user UDC-based PNC, the key issue is to find M-user UDCs. This paper explores the UDC proposed by [45], which provides two codewords $\mathbf{x}_m$ and $\mathbf{y}_m$ for the mth user. Thus, its sum rate, $R_{\mathrm{sum}} = \frac{1}{n}\log_2 \prod_{m=1}^{M} 2 = M/n$.

Set $\mathbf{z}_m = \mathbf{x}_m - \mathbf{y}_m$, where $\mathbf{z}_m \in \{0,-1,1\}$. Define an $M \times n$ difference matrix, $\mathbf{D}$, for the M users' codeword set $(C_1, C_2, \ldots, C_M)$, which contains $\mathbf{z}_m$ as a row. Let the rows of $\mathbf{D}$ be linearly independent over $\{0,-1,1\}$. For an arbitrary integer l $(1 \le l \le n)$, if the lth component of z_m is 0, then the lth components of $\mathbf{x}_m$ and $\mathbf{y}_m$ both equal to 0. If the lth component of $\mathbf{z}_m$ is 1 (or -1), then the lth components of $\mathbf{x}_m$ and $\mathbf{y}_m$ are 1 and 0 (or 0 and 1), respectively. The initial value of $\mathbf{D}$ is $\mathbf{D}_0 = [1]$, and the iterative procedure for computing the difference matrix $\mathbf{D}$ is given as

$$\mathbf{D}_b = \begin{bmatrix} \mathbf{D}_{b-1} & \mathbf{D}_{b-1} \\ \mathbf{D}_{b-1} & -\mathbf{D}_{b-1} \\ \mathbf{I}_{b-1} & \mathbf{0}_{b-1} \end{bmatrix} \tag{21}$$

where $\mathbf{I}_{b-1}$ is the identity matrix of order of 2^{b-1}, $\mathbf{0}_{b-1}$ is the zero matrix of order of 2^{b-1}, and b is the order of the difference matrix $\mathbf{D}$. When $b = 1$ and suppose there are three users, then we have

$$\mathbf{D}_b = \begin{bmatrix} \mathbf{1} & \mathbf{1} \\ \mathbf{1} & -\mathbf{1} \\ \mathbf{1} & \mathbf{0} \end{bmatrix}. \tag{22}$$

Thus, the codeword set of each user is $C_1 = \{11, 00\}$, $C_2 = \{10, 01\}$, and $C_3 = \{10, 00\}$. If each user uses QPSK modulation, the mapping set at the relay is illustrated in Fig. 9.

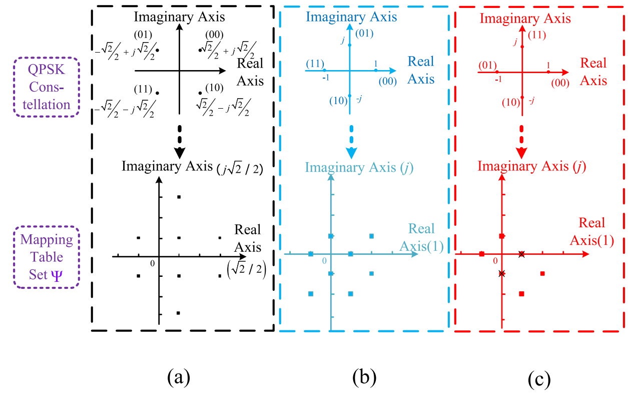

Fig. 9. Different QPSK constellations and mapping sets, Ψ, at the relay node with three users.

There are some elements overlapping in case (*c*) because of different QPSK constellation, which makes the codewords no longer uniquely decodable. Moreover, the elements in set Ψ vary with different constellation mappings in cases (*a*) and (*b*), thereby resulting in varying Euclidean distances. The minimum Euclidean distances for cases (a) and (b) are 2 and $\sqrt{2}$, respectively. So, assuming BPSK modulation, the mapping relationship is presented in Table V.

TABLE V
CODING AND BPSK MODULATION MAPPING FOR THREE USERS

C_1	{00 , 11}	S_1	{ -1-1 ,11 }
C_2	{01 , 10}	S_2	{ -11 ,1-1 }
C_3	{00 , 10}	S_3	{ -1-1 ,1-1 }

The subsequent analytical process is similar to that of the 2-user case, and is thus omitted for brevity purposes.

B. Pre-Coding for the Proposed Scheme

As discussed in the preceding parts, the SER of the system is affected by the optimum decision threshold as shown in (6), which is a function of the channel impulse response, h_1 (or h_2). Consequently, the BER and the capacity of the system vary with the channel impulse response. This part will discuss pre-coding for the proposed schemes in an attempt to reduce the effect of the channel impulse response. The system diagram with pre-coding is illustrated in Fig. 10.

The main difference lies in the addition of a pre-coding processor inserted before transmission. If the CSI is known at each user terminal, the weights w_1 and w_2 for users 1 and 2 should be

$$\begin{cases} w_1 = \frac{h_1^*}{|h_1|^2} \\ w_2 = \frac{h_2^*}{|h_2|^2}. \end{cases} \tag{23}$$

Thus, the received signal becomes

$$\begin{aligned} r(t) &= h_1\left(w_1 s_1(t)\right) + h_2\left(w_2 s_2(t)\right) + n(t) \\ &= h_1 \frac{h_1^*}{|h_1|^2} s_1(t) + h_2 \cdot \frac{h_2^*}{|h_2|^2} s_2(t) + n(t) \\ &= s_1(t) + s_2(t) + n(t) \end{aligned} \tag{24}$$

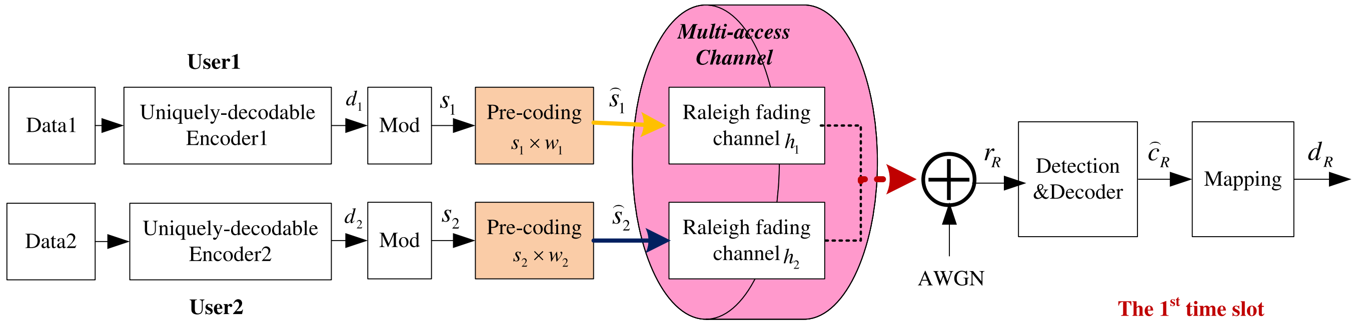

Fig. 10. Pre-coding for the proposed UDC-based PNC schemes.

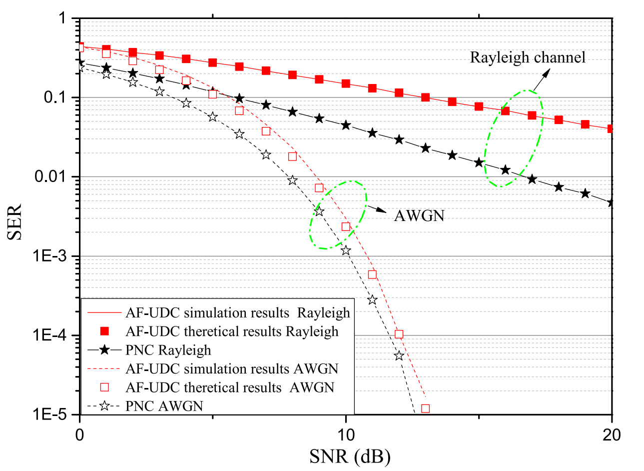

Fig. 11. SER performances of the AF UDC-based PNC mode both in Rayleigh flat fading and AWGN channels, where $C_1 = \{00, 11\}$ and $C_2 = \{00, 01, 10\}$.

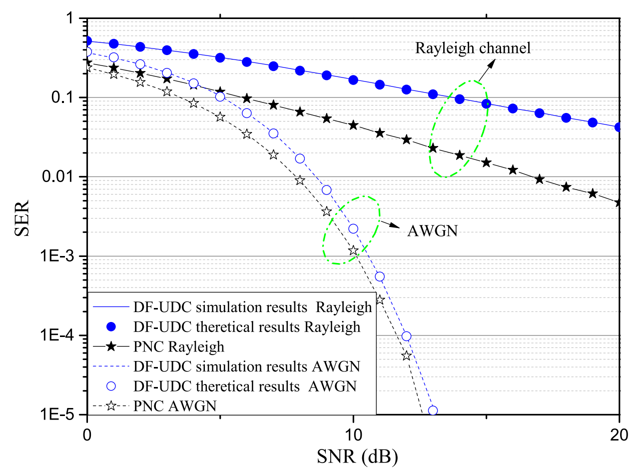

Fig. 12. SER performances of the DF UDC-based PNC mode both in Rayleigh flat fading and AWGN channels, where $C_1 = \{00, 11\}$ and $C_2 = \{00, 01, 10\}$.

where $x = 2\sqrt{E_c}$, and $y = 0$. As can be seen from (21), the effect of flat fading is removed, and the channel becomes an AWGN equivalent one.

Pre-coding is useful in improving the system performance under the fading channel. However, the CSI needs to be known at the user terminals as well as at the relay node, along with a feedback link. The extra feedback channel increases the complexity of the system. Thus, channel estimation is also an interesting issue for the proposed schemes, which is beyond the scope of this paper.

VI. Simulation Results

This section presents computer simulation results to validate both the SER and throughput performances of the proposed schemes.

A. SER Performance

It is assumed that $\sigma^2_{\text{Ray}} = 1$, and the UDC shown in Table I is used for the $M = 2$ case. Figs. 11–13 plot the SER results of users 1 and 2 with different transmission modes. For fair comparison, each node (a user terminal or the relay node) is allocated the same transmit power.

As can be observed from Figs. 11 and 12, the SER performances of the proposed systems in Rayleigh fading channels are worse than those in AWGN channels. And, the traditional PNC provides the best SER performances among the AF and DF modes. Moreover, the theoretical results are almost in agreement with the simulated results in both the AWGN and Rayleigh fading channels. From Fig. 13, it is found that the DF mode offers a slightly better SER performance than that of the AF mode, since UDC is employed at both the user terminals and the relay node, which enables error detection (or correction) at all the nodes.

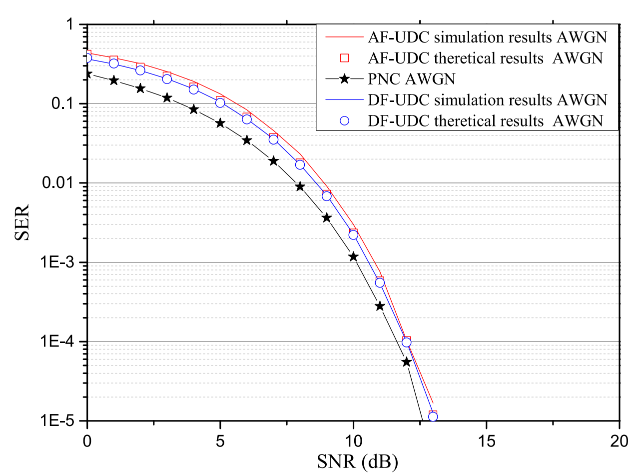

Fig. 13. Comparison between the AF and DF modes in AWGN channels, where $C_1 = \{00, 11\}$ and $C_2 = \{00, 01, 10\}$.

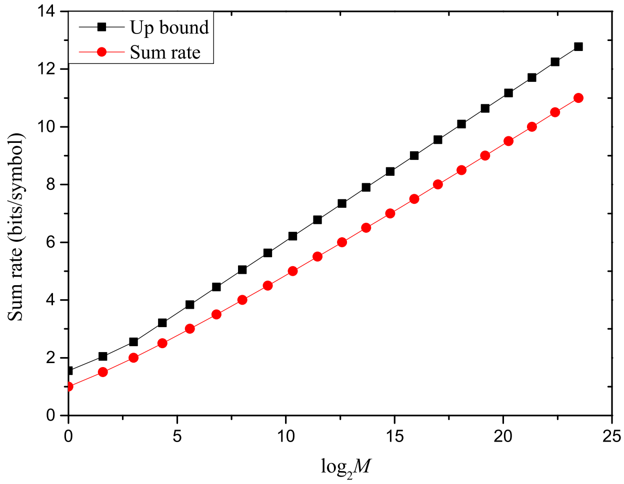

Fig. 14. Sum rate of the different UDC construction method, where M is the number of users.

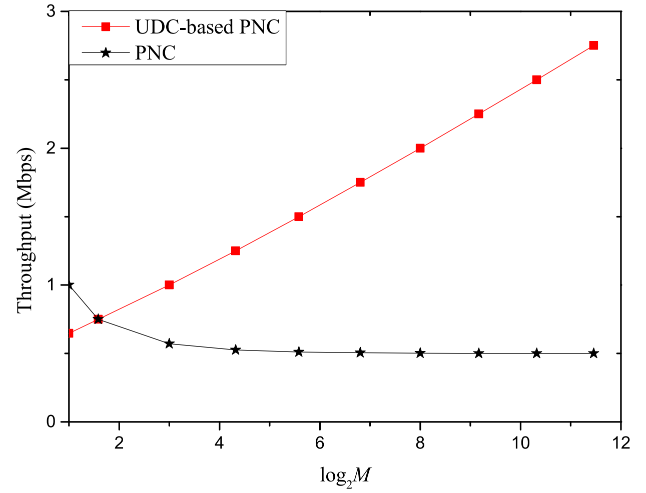

Fig. 15. Throughput comparison between the UDC-based PNC and the classical PNC.

With the increasing of SNR, the difference between the AF and DF modes becomes smaller. By contrast, the AF mode exhibits a worse SER performance since the UDC is not used at the relay node. As for the AWGN channels, the SER performances are comparable to that of the PNC system.

B. Throughput

In this paper, the throughput TP is defined as the number of bits successfully transmitted by the system per unit TS. Attributed to the properties of UDCs, the proposed schemes need only two TSs for complete information exchange, irrespective of the number of users in the system. As a result, given the sum rate of UDC, R_{sum}, the throughputs under the AF (TP_{AF}) and DF (TP_{DF}) modes can be expressed, respectively, as

$$\begin{aligned} \text{TP}_{\text{AF}} &= R_{\text{sum}} R_s (1 - P_{e,\text{AF}})/2, \\ \text{TP}_{\text{DF}} &= R_{\text{sum}} R_s (1 - P_{e,\text{DF}})/2 \end{aligned} \tag{25}$$

where $P_{e,\text{AF}}$ (or $P_{e,\text{DF}}$) is the BER of the proposed scheme, and R_s is the symbol rate. Let R_s be 10^6 symbol/s, and assume $P_{e,\text{AF}} = P_{e,\text{DF}} = 0$. Thus, the maximum throughput of the UDC-based PNC is $\text{TP}_{\text{UDC}} = R_{\text{sum}}/2$ Mb/s.

For the given simple UDC for two users (as shown in Table I), $\text{TP}_{\text{UDC}} = 1.2925/2 = 0.6462$ Mb/s.

According to the different UDC construction method, its sum rate, $R_{\text{sum}} = M/n$, where $M = (b+2)\cdot 2^{b-1}$ and $n = 2^b$, as shown in Fig. 14. Thus, the maximum throughput is $\text{TP}_{\text{UDC}} = \frac{M}{2n}$ Mb/s. For example, when $M = 3$ and $n = 2$, its throughput is 0.75 Mb/s; when $M = 8$ and $n = 4$, the throughput equals 1 Mb/s. Obviously, the throughput of UDC-based PNC is an increasing function of M.

Since the PNC with M users needs $2M - 2$ TSs to exchange information, the system throughput is given as

$$\text{TP}_{\text{PNC}} = \frac{M R_s (1 - P_{e,\text{PNC}})}{2M - 2} \tag{26}$$

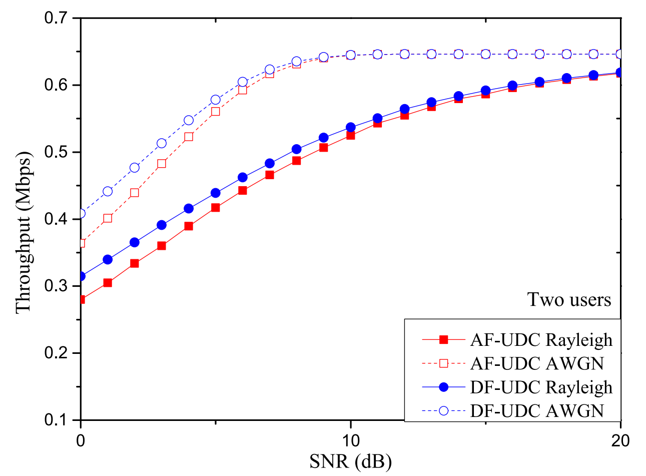

Fig. 16. System throughput of various comparative schemes with the AF and DF modes.

where $P_{e,\text{PNC}}$ is the BER of the M-user PNC system. Obviously, (26) is a decreasing function of M. When $M = 2$, the PNC system has the maximum throughput of $\text{TP}_{\text{PNC}} = 1$ Mb/s. When $M \to \infty$, $\text{TP}_{\text{PNC}} = 0.5$ Mb/s.

The throughputs of the UDC-based PNC and the classical PNC are compared in Fig. 15. When $M = 2$, the throughput of the UDC-based PNC is smaller than that of the PNC system. When $M \geq 3$, the throughput of the UDC-based PNC is equal to or larger than that of the PNC system. With the increase in M, the UDC-based PNC provides a better throughput performance than that by the classical PNC system.

Fig. 16 plots the system throughput of various schemes with both the AF and DF modes. From the figure, it can be seen that for any transmission scheme, if the SNR is large enough, its throughput in the AWGN channel is always higher than that in the Rayleigh fading channel. However, with an increase in the SNR, the discrepancy becomes smaller. And, if the SNR is large enough, the throughputs in the AWGN and the Rayleigh fading channels will be around the same. For all the schemes in the

AWGN channel, it is found that the DF mode provides a higher throughput than that by its AF counterpart, since its SER in the multiple-access channel is smaller than that in the AF mode.

VII. Conclusion

This paper proposed new UDC-based PNC schemes for wireless cooperative communications, which extract and map data from different users at the relay node. It is capable of reducing the number of TSs for the M-node network, and thus, improves the system throughput. This paper also introduced two transmission schemes, i.e., the AF and DF modes, both of which provide different features. For example, the AF mode is relatively easy to implement, but offers a poorer SER performance. A notable advantage of the proposed UDC-based PNC schemes is that they work effectively in the flat fading channel with a small SER penalty. Therefore, the proposed schemes will be very useful for future wireless communications systems. There still remain some open and interesting problems for the proposed schemes, e.g., multiple-user UDC design, which will be studied in our future work.

Acknowledgment

The authors would like to thank Prof. Shu Lin, University of California at Davis, Davis, CA, USA, for providing insightful comments to greatly help improve this manuscript.

References

[1] S. R. Li, R. W. Yeung, and N. Cai, "Linear network coding," *IEEE Trans. Inf. Theory*, vol. 49, no. 2, pp. 371–381, Feb. 2003.

[2] S. Zhang, S. C. Liew, and P. P. Lam, "Physical-layer network coding," in *Proc. Int. Conf. Mobile Comput. Netw.*, Los Angeles, CA, USA, Sep. 2006, pp. 358–365.

[3] P. Popovski and H. Yomo, "The anti-packets can increase the achievable throughput of a wireless multi-hop network," in *Proc. IEEE Int. Conf. Commun.*, Istanbul, Turkey, May 2006, pp. 3885–3890.

[4] T. P. Do, J. S. Wang, I. Song, and Y. H. Kim, "Joint relay selection and power allocation for two-way relaying with physical layer network coding," *IEEE Commun. Lett.*, vol. 17, no. 2, pp. 301–304, Feb. 2013.

[5] S. Fu, K. Lu, T. Zhang, Y. Qian, and H. Chen, "Cooperative wireless networks based on physical layer network coding," *IEEE Wireless Commun.*, vol. 17, no. 6, pp. 86–95, Dec. 2010.

[6] A. Thampi, S. C. Liew, S. Armour, Z. Fan, L. You, and D. Kaleshi, "Physical-layer network coding in two-way heterogeneous cellular networks with power imbalance," *IEEE Trans. Veh. Technol.*, vol. 65, no. 11, pp. 9072–9084, Nov. 2016.

[7] P. Chen, K. Su, Y. Fang, and L. Kong, "The design of protograph LDPC codes for channel-coded physical-layer network coding," in *Proc. IEEE 27th Annu. Int. Symp. Pers., Indoor, Mobile Radio Commun.*, Valencia, Spain, Sep. 2016, pp. 1–6.

[8] Y. Zhao, M. Johnston, C. Tsimenidis, and L. Chen, "Non-binary turbo-coded physical-layer network coding on impulsive noise channels," *Electron. Lett.*, vol. 52, no. 24, pp. 1984–1986, Nov. 2016.

[9] S. Zhang and S. C. Liew, "Channel coding and decoding in a relay system operated with physical-layer network coding," *IEEE J. Sel. Areas Commun.*, vol. 27, no. 5, pp. 788–796, Jun. 2009.

[10] U. Bhat and T. M. Duman, "Decoding strategies at the relay with physical-layer network coding," *IEEE Trans. Wireless Commun.*, vol. 11, no. 12, pp. 4503–4513, Dec. 2012.

[11] F. D. Zahra and P. Mitran, "On non-binary constellations for channel-coded physical-layer network coding," *IEEE Trans. Wireless Commun.*, vol. 12, no. 1, pp. 312–319, Jan. 2013.

[12] D. To and J. Choi, "Convolutional codes in two-way relay networks with physical-layer network coding," *IEEE Trans. Wireless Commun.*, vol. 9, no. 9, pp. 2724–2729, Sep. 2010.

[13] J. Liu, M. Tao, and Y. Xu, "Pairwise check decoding for LDPC coded two-way relay block fading channels," *IEEE Trans. Commun.*, vol. 60, no. 8, pp. 2065–2076, Aug. 2012.

[14] H. Pan, L. Lu, and S. C. Liew, "Network-coded multiple access with high-order modulations," *IEEE Trans. Veh. Technol.*, vol. 66, no. 11, pp. 9776–9792, Jun. 2017.

[15] Q. Yu, D. Zhang, H. Chen, and W. Meng, "Physical layer network coding systems with M-ary FSK modulation," *IEEE Trans. Veh. Technol.*, vol. 65, no. 1, pp. 204–213, Jan. 2016.

[16] H. J. Yang, Y. Choi, and J. Chun, "Modified high-order PAMs for binary coded physical-layer network coding," *IEEE Commun. Lett.*, vol. 14, no. 8, pp. 689–691, Aug. 2010.

[17] M. Ju and I. Kim, "Error performance analysis of BPSK modulation in physical-layer network-coded bidirectional relay networks," *IEEE Trans. Commun.*, vol. 58, no. 10, pp. 2770–2775, Oct. 2010.

[18] P. Chen, S. Liew, and L. Shi, "Bandwidth-efficient coded modulation schemes for physical-layer network coding with high-order modulations," *IEEE Trans. Commun.*, vol. 65, no. 1, pp. 147–160, Jan. 2017.

[19] L. Guo, Z. Ning, Q. Song, Y. Cui, and Z. Chen, "Toward efficient 5G transmission: SER performance analysis for asynchronous physical-layer network coding," *IEEE Access*, vol. 4, no. 99, pp. 5083–5097, Sep. 2016.

[20] S. Chang and B. Kelley, "An efficient time synchronization scheme for broadband two-way relaying networks based on physical-layer network coding," *IEEE Commun. Lett.*, vol. 16, no. 9, pp. 1416–1419, Sep. 2012.

[21] L. Lu and S. C. Liew, "Asynchronous physical-layer network coding," *IEEE Trans. Wireless Commun.*, vol. 11, no. 2, pp. 819–831, Feb. 2012.

[22] X. Wu, C. Zhao, and X. You, "Joint LDPC and physical-layer network coding for asynchronous bi-directional relaying," *IEEE J. Sel. Areas Commun.*, vol. 31, no. 8, pp. 1446–1454, Aug. 2013.

[23] H. Zhang and L. Cai, "Bi-directional multi-hop wireless pipeline using physical-layer network coding," *IEEE Trans. Wireless Commun.*, vol. 16, no. 12, pp. 7950–7965, Dec. 2017.

[24] A. Akhtar, M. Nakhai, and A. Aghvami, "On the use of cooperative physical layer network coding for energy efficient routing," *IEEE Trans. Commun.*, vol. 61, no. 4, pp. 1498–1509, Apr. 2013.

[25] P. Liu, S. Gazor, and I. M. Kim, "An opportunistic protocol employing independent codebooks for bidirectional cooperative networks," *IEEE Trans. Veh. Technol.*, vol. 62, no. 2, pp. 902–908, Feb. 2013.

[26] A. Schmidt, R. Schober, and W. Gerstacker, "Nonlinear equalization approaches for physical layer network coding," *IEEE Trans. Wireless Commun.*, vol. 16, no. 2, pp. 825–838, Feb. 2017.

[27] D. Luo, Q. Yu, and W. Meng, "Optimum power allocation for OFDM in physical-layer network coding over a flat frequency-selective fading channel," in *Proc. 9th Int. Conf. Inf., Commun. Signal Process.*, Tainan, Taiwan, Dec. 2013, pp. 1–5.

[28] D. Luo, Q. Yu, W. Meng, and C. Li, "Pre-coding for multi-user physical network coding over a flat fading channel," in *Proc. IEEE Global Commun. Conf.*, Austin, TX, USA, Dec. 2014, pp. 4366–4370.

[29] T. Yang, X. Yuan, L. Ping, I. B. Collings, and J. Yuan, "A new physical-layer network coding scheme with eigen-direction alignment precoding for MIMO two-way relaying," *IEEE Trans. Commun.*, vol. 61, no. 3, pp. 973–986, Mar. 2013.

[30] S. Zhang and S. C. Liew, "Physical layer network coding with multiple antennas," in *Proc. IEEE Wireless Commun. Netw. Conf.*, Sydney, Australia, Apr. 2010, pp. 1–6.

[31] L. Yang, T. Yang, Y. Xie, J. Yuan, and J. An, "Linear physical-layer network coding and information combining for the K-user fading multiple-access relay network," *IEEE Trans. Wireless Commun.*, vol. 15, no. 8, pp. 5637–5650, Aug. 2016.

[32] H. Pan, L. Lu, and S. C. Liew, "Practical power-balanced non-orthogonal multiple access," *IEEE J. Sel. Areas Commun.*, vol. 35, no. 10, pp. 2312–2327, Jul. 2017.

[33] J. Li, W. Chen, Z. Lin, and B. Vucetic, "Design of physical layer network coded LDPC code for a multiple-access relaying system," *IEEE Commun. Lett.*, vol. 17, no. 4, pp. 749–752, May 2013.

[34] L. You, S. Liew, and L. Lu, "Network-coded multiple access II: Toward real-time operation with improved performance," *IEEE J. Sel. Areas Commun.*, vol. 33, no. 2, pp. 264–280, Dec. 2015.

[35] H. H. J. Liao, "Multiple access channels," Ph.D. dissertation, Dept. Elect. Eng., Univ. Hawaii, Honolulu, HI, USA, 1972.

[36] T. Kasami and S. Lin, "Coding for a multiple-access channel," *IEEE Trans. Inf. Theory*, vol. 22, no. 2, pp. 129–137, Mar. 1976.

[37] T. Kasami and S. Lin, "Bounds on the achievable rates of block coding for a memoryless multiple-access channel," *IEEE Trans. Inf. Theory*, vol. 24, no. 2, pp. 187–197, Mar. 1978.

[38] T. Kasami, S. Lin, V. Wei, and S. Yamamura, "Graph theoretic approaches to the code construction for the two-user multiple-access binary adder channel," *IEEE Trans. Inf. Theory*, vol. 29, no. 1, pp. 114–130, Jan. 1983.
[39] H. V. Tilborg, "Upper bounds on $|C_2|$ for a uniquely decodable code pair (C_1, C_2) for a two-access binary adder channel," *IEEE Trans. Inf. Theory*, vol. 29, no. 3, pp. 386–389, May 1983.
[40] P. Vanroose and E. C. Meulen, "Uniquely decodable codes for deterministic relay channels," *IEEE Trans. Inf. Theory*, vol. 38, no. 4, pp. 1203–1212, Jul. 1992.
[41] D. B. Jevtic, "Disjoint uniquely decodable codebooks for noiseless synchronized multiple-access adder channels generated by integer sets," *IEEE Trans. Inf. Theory*, vol. 38, no. 3, pp. 1142–1146, May 1992.
[42] S. C. Chang and E. J. Weldon, "Coding for a T-user multiple access channel," *IEEE Trans. Inf. Theory*, vol. 25, no. 5, pp. 684–691, Sep. 1979.
[43] L. Kiviluoto and P. R. J. Ostergard, "New uniquely decodable codes for the T-user binary adder channel with $3 \leq T \leq 5$," *IEEE Trans. Inf. Theory*, vol. 53, no. 3, pp. 1219–1220, Mar. 2007.
[44] S. I. Bross and I. F. Blake, "Upper bound for uniquely decodable codes in a binary input N-user adder channel," *IEEE Trans. Inf. Theory*, vol. 44, no. 1, pp. 334–340, Jan. 1998.
[45] K. Michel and D. A. Pados, "Uniquely decodable code-division via augmented Sylvester–Hadamard matrices," in *Proc. IEEE Wireless Commun. Netw. Conf.*, Paris, France, Apr. 2012, pp. 359–363.
[46] W. E. Ryan and S. Lin, *Channel Codes: Classical and Modern*. Cambridge, U.K.: Cambridge Univ. Press, 2009.
[47] Y. Li, Q. Yu, K. He, and W. Xiang, "Apply uniquely-decodable codes to multiuser physical-layer network coding based on amplify-and-forward criterion," in *Proc. IEEE Global Commun. Conf.*, San Diego, CA, USA, Dec. 2015, pp. 1–6.

Qi-Yue Yu (M'08–SM'17) received the B.Eng., M.Eng., and Ph.D. degrees from the Harbin Institute of Technology (HIT), Harbin, China, in 2004, 2006, and 2010, respectively.

She is currently a Full Professor with the School of Electronics and Information Engineering, HIT. During Apr. 2007–Mar. 2008, she studied in Adachi Lab, Tohoku University, Japan and was a Research Assistant with Tohoku University Global COE Program. In 2010, she was invited to the City University of Hong Kong to research on multi-user MIMO technology. She was invited to the University of Southern Queensland to conduct researches on distributed antenna systems in January–March 2014. During September 2015–September 2016, she was a Visiting Scholar with the University of California, Davis, CA, USA. Her research interests include modulation and coding, information theory, and multi-access techniques and MIMO for broadband wireless communications.

Ya-Tian Li received the B. Eng. and M. Eng. degrees in communications engineering from the Harbin Institute of Technology (HIT), Harbin, China, in 2013 and 2015, respectively. He is currently working toward the Ph.D. degree in mechanical electrical engineering at the University of Chinese Academy of Sciences (UCAS), Beijing, China.

Also, he is currently a Research Assistant with the Laboratory of Laser Communication, Changchun Institute of Optics, Fine Mechanics and Physics (CIOMP), Chinese Academy of Sciences (CAS), Changchun, China. His research interests include free space optics and wireless communications.

Wei-Xiao Meng (SM'10) received the B.Eng., M.Eng., and Ph.D. degrees from the Harbin Institute of Technology (HIT), Harbin, China, in 1990, 1995, and 2000, respectively.

From 1998 to 1999, he was a Senior Visiting Researcher with the NTT DoCoMo, where he was involved in adaptive array antenna and dynamic resource allocation for beyond 3G. He is now a Full Professor and the Vice Dean with the School of Electronics and Information Engineering, HIT. He has authored or coauthored 4 books and more than 260 papers in journals and international conferences. His research interests include broad-band wireless communications, space–air–ground integrated networks, and wireless localization technologies.

Prof. Meng is the Chair of the IEEE Communications Society Harbin Chapter, a Fellow of the China Institute of Electronics, and a Senior Member of the IEEE ComSoc and the China Institute of Communication. He was an Editorial Board Member for Wiley's journal, *Wireless Communications and Mobile Computing*, from 2010 to 2017, an Area Editor for the *Physical Communication* from 2014 to 2016, an Editorial Board for the IEEE COMMUNICATIONS SURVEYS AND TUTORIALSfrom 2014 to 2017 and the IEEE WIRELESS COMMUNICATIONSsince 2015. He was the Leading TPC Co-Chair of the ChinaCom2011 and the ChinaCom2016, the Leading Services and Applications Track Co-Chair of the IEEE WCNC2013, Awards Co-Chair of the IEEE ICC2015, the Wireless Networking Symposia Co-Chair of the IEEE Globecom2015, the AHSN Symposia Co-Chair of the IEEE Globecom2018, and the Leading Workshop Co-Chair of the IEEE ICC2019. In 2005, he was honored provincial excellent returnee and selected into the New Century Excellent Talents (NCET) Plan by the Ministry of Education, China in 2008, and the Distinguished Academic Leadership of Harbin. He was the recipient of the Chapter of the Year Award, the Asia Pacific Region Chapter Achievement Award, and the Member and Global Activities Contribution Award in 2018.

Wei Xiang (S'00–M'04–SM'10) received the B.Eng. and M.Eng. degrees, both in electronic engineering, from the University of Electronic Science and Technology of China, Chengdu, China, in 1997 and 2000, respectively, and the Ph.D. degree in telecommunications engineering from the University of South Australia, Adelaide, S. Aust., Australia, in 2004. He has authored or coauthored more than 250 peer-reviewed papers with more than 130 journal articles. His research interest include the broad areas of communications and information theory, particularly the Internet of Things, and coding and signal processing for multimedia communications systems.

During 2004–2015, he was with the School of Mechanical and Electrical Engineering, University of Southern Queensland, Queens., Australia. He is currently the Founding Professor and the Head of Discipline of Internet of Things Engineering, James Cook University, Cairns, Queens., Australia.

Prof. Xiang is an Elected Fellow of the IET in UK and Engineers Australia. He was the recipient of the TNQ Innovation Award in 2016, and Pearcey Entrepreneurship Award (highly commended) in 2017, and the Engineers Australia Cairns Engineer of the Year in 2017. He was a co-recipient of three Best Paper awards at 2015 WCSP, 2011 IEEE WCNC, and 2009 ICWMC. He has been a recipient of several prestigious fellowship titles. He was named a Queensland International Fellow (2010–2011) by the Queensland Government of Australia, an Endeavour Research Fellow (2012–2013) by the Commonwealth Government of Australia, a Smart Futures Fellow (2012–2015) by the Queensland Government of Australia, and a JSPS Invitational Fellow jointly by the Australian Academy of Science and Japanese Society for Promotion of Science (2014–2015). He is the Vice Chair of the IEEE Northern Australia Section. He was an Editor for the IEEE COMMUNICATIONS LETTERS (2015–2017), and is an Associate Editor for Springer's *Telecommunications Systems*. He has worked in a large number of international conferences in the capacity of General Co-Chair, TPC Co-Chair, Symposium Chair, etc. Because of his instrumental leadership in establishing Australia's first Internet of Things Engineering degree program, he was selected into the Pearcy Foundations Hall of Fame in October 2018.